# 716

HIGH RESOLUTION UV AND VISIBLE SOLAR ATLAS

MS-13C

No New I.D. Recorded

Table of Contents

1. Introduction

2. Errata/Change Log

3. LINKS TO RELEVANT INFORMATION IN THE ONLINE NSSDC INFORMATION SYSTEM

4. Catalog Materials

    a. Associated Documents

    b. Core Catalog Materials

---

## 1. INTRODUCTION:

The documentation for this data set was originally on paper, kept in NSSDC's Data Set Catalogs (DSCs). The paper documentation in the Data Set Catalogs have been made into digital images, and then collected into a single PDF file for each Data Set Catalog. The inventory information in these DSCs is current as of July 1, 2004. This inventory information is now no longer maintained in the DSCs, but is now managed in the inventory part of the NSSDC information system. The information existing in the DSCs is now not needed for locating the data files, but we did not remove that inventory information.

The offline tape datasets have now been migrated from the original magnetic tape to Archival Information Packages (AIP's).

A prior restoration may have been done on data sets, if a requestor of this data set has questions; they should send an inquiry to the request office to see if additional information exists.

2. ERRATA/CHANGE LOG:

NOTE: Changes are made in a text box, and will show up that way when displayed on screen with a PDF reader.

***When printing, special settings may be required to make the text box appear on the printed output.***

| Version | Date | Person | Page | Description of Change |
|---|---|---|---|---|
| 01 | | | | |
| 02 | | | | |

3 LINKS TO RELEVANT INFORMATION IN THE ONLINE NSSDC INFORMATION SYSTEM:

http://nssdc.gsfc.nasa.gov/nmc/

[NOTE: This link will take you to the main page of the NSSDC Master Catalog. There you will be able to perform searches to find additional information]

4. CATALOG MATERIALS:

a. Associated Documents To find associated documents you will need to know the document ID number and then click here. http://nssdcftp.gsfc.nasa.gov/miscellaneous/documents/

b. Core Catalog Materials

High Resolution UV and Visible Solar Atlas

MS-13C

No New I.D. Recored

The Dataset consists of one 9-track 6250 bpi tape. The data are written in ASCII in one file. The 'D' and 'C' numbers follow:

D-80379 C-28059

MS-13C

# A HIGH RESOLUTION SOLAR ATLAS FOR FLUORESCENCE CALCULATIONS

Michael F. A'Hearn

John T. Ohlmacher

and

David G. Schleicher

Technical Report: TR AP83-044

29 July 1983

UNIVERSITY OF MARYLAND
DEPARTMENT OF PHYSICS AND ASTRONOMY
COLLEGE PARK, MARYLAND

$$\frac{\Delta\lambda}{\lambda} = \frac{1}{3\times10^5}$$

for $3000\,A^\circ$

$$\Delta\lambda = \frac{1}{100}\,A^\circ$$

# A HIGH RESOLUTION SOLAR ATLAS FOR FLUORESCENCE CALCULATIONS

Michael F. A'Hearn

John T. Ohlmacher

and

David G. Schleicher

Technical Report: TR AP83-044

29 July 1983

Astronomy Program

University of Maryland

College Park, MD 20942

USA

# I. INTRODUCTION

In the course of our program to study the fluorescence process in comets, we frequently require the solar spectrum at high spectral resolution in absolute units. For some programs, such as fluorescence of hydrogen in the Lyman-$\alpha$ line, only a small portion of the solar spectrum is needed, e.g., the few Angstroms including the Lyman-$\alpha$ line. At the other extreme, however, are molecules like $C_2$ and $CO^+$. These species have emission bands which extend from the ultraviolet to the red ($CO^+$) or even to the infrared ($C_2$). A proper calculation of the fluorescence by these molecules thus requires a homogeneous solar spectrum over this entire spectral range. In order to meet this need we have synthesized a solar spectrum from various sources.

There are a number of characteristics required in a solar atlas to be used for fluorescence calculations. In the first place, the spectrum must refer to the whole disc of the sun (i.e., the solar irradiance), not just the center of the sun. Secondly it must have a reasonably good calibration in absolute flux units. Thirdly, it must have a spectral resolution comparable to or better than the thermal widths expected for cometary specral lines and, in order to study the Greenstein effect in comets, the spectral resolution of the atlas must be better than the expected Doppler widths due to mass motions within the comet. The overall expansion of cometary material is expected to take place at velocities of order 1 km/sec while the expected sublimation temperatures, 150 to 200 K, imply thermal velocities of several tenths of a km/sec. Therefore, a spectral resolution of several tenths of a km/sec is appropriate for our purposes. This turns out to require unavailable data. Fortunately for us, the solar rotation (2 km/sec near the equator) smooths out all features finer than this. We can therefore accept a somewhat lower resolution, of order 1 km/sec, provided it is interpolated to better than 1 km/sec.

Our general approach has been to provide an absolute intensity calibration which is completely independent of the high resolution data which form the basis for our final spectrum. Several sources of low resolution data have been combined to provide an absolutely calibrated spectrum from 2250 Å to 7000 Å. Similarly three different sources of high resolution data are used to cover this same spectral range. We have used the low resolution data to put each high resolution spectrum on an absolute scale. We have then combined the three high resolution spectra in their overlap regions to produce a single, absolutely calibrated high resolution spectrum over the entire spectral range.

Although this atlas was assembled for our own purposes of calculating the fluorescence spectrum in comets, it does have other applications. Nicolet (1981), for example, has recently discussed the same problem from the viewpoint of photochemical rates relevant to aeronomy although he did not require spectral resolution nearly as high as ours. Similarly, these results are needed for fluorescence calculations relevant to planetary atmospheres and exospheres.

## II. SOLAR VARIABILIY

An important question is whether or not the solar spectrum shows any variability that would matter for our purposes.

The only fluctuations which matter for our purposes are those which exceed a few percent on time scales from hours (the time required to establish fluorescent equilibrium for cometary species) to several decades (the time span of quantitative data on comets). Two recent conferences on solar variability* have considered many different types of variation. Examination of the proceedings leads one to conclude that, at least in the optical region, there are no changes in the solar spectrum relevant to our interests with the exception of changes in a few discrete absorption lines. For example, the intensity at the core of the Ca II K line does vary significantly with the solar cycle (Livingston, et al. 1981). Since this will matter only for transitions pumped at that frequency, none of which are of interest to us, we have ignored this effect. Fluctuations associated with the five minute oscillations (e.g., Fröhlich, 1981) are too rapid to be of interest to us.

In the ultraviolet, there are large (>30%) discrepancies among different observers. Simon (1981) has reviewed the various determinations, looking specifically for real variations. The best results should come from repeated measurements with the same instrument, such as those of Simon himself. He concludes that the variations with solar rotation (27-day period) are 1-2% for $\lambda$2400 - 3300 Å (mainly at the discrete Fraunhofer lines of Mg II near 2800 Å) and 2-4% for $\lambda$2000 - 2400 Å (mainly shortward of $\lambda$2100 Å). These fluctuations are only of marginal significance for our purposes and the largest ones are

*XIVth ESLAB Symposium on "Physics of Solar Variations" Sept. 1980: Papers published as vol. 74 of Solar Physics. Workshop held at Goddard Space Flight Center Nov. 1980: Proceedings published as "Variations of the Solar Constant" ed. S. Sofia NASA Conf. Publ. 2191.

outside the spectral range under consideration (i.e., $\lambda < 2250$ Å). We will therefore neglect these changes. The longer term variability, specifically that with the 11-year solar cycle, is less well determined. Simon therefore gives only upper limits of 2% for the region $\lambda 2400 - 3300$ Å and 10% for the region $\lambda 2000 - 2400$ Å. Again the variation longward of $\lambda 2400$ is of only marginal significance and we neglect it. The upper limit for variations in the range $\lambda 2000 - 2400$ Å might be important for our purposes, but it is clear that with current data we cannot take these variations into account since they are not adequately determined.

In summary, the present atlas will make no attempt to take into account any variations with time. Such variations may be significant, however, at the core of certain lines such as the K-line and at wavelengths < 2400 Å. These limitations must be kept in mind when using the atlas.

## III. ABSOLUTE FLUX CALIBRATIONS

The absolute calibration of the solar irradiance in the optical region has been taken from the work of Neckel and Labs (1981). They have provided the total irradiance at 1 AU integrated over 20 Å-wide bandpasses (20.5 Å-wide for $\lambda < 4010$ Å). They have estimated the accuracy of their results as better than 1% at most wavelengths and better than 2% in the near ultraviolet. Other absolute spectra of the sun, however, differ from these results by much more than 2%. The choice of the data from Neckel and Labs is strongly supported by the work of Hardorp (1980). He has discussed in some detail the comparison between the sun and other stars which resemble the sun, both in respect to the overall flux distribution and also in the strength of two discrete absorption features in the near ultraviolet region of the spectrum. The earlier calibration by Labs and Neckel (1968) was the only solar spectrum which could match the overall flux distribution of any stars which had the solar strength for the discrete features. In the course of that investigation, Hardorp uncovered the small errors in their flux distribution which have been corrected in the more recent work by Neckel and Labs. Although there may be uncertainties larger than those cited by Neckel and Labs, it seems clear to us that these data are by far the best available and that consequently there is no point in averaging them with any other data.

In the ultraviolet, the situation is more ambiguous. The discrepancies among different observers are larger and there is less basis for choosing one over another. In their review of this quesion some years ago, Smith and Gottlieb (1974) chose the work of Broadfoot (1972) as the best, but many more recent sources of data are now available.

Since the discrepancies among different observers of the ultraviolet flux distribution of the sun are much larger than the real variations, we must

select among the observers. In the spectral region λ2500 - 3000 Å, the data of Broadfoot (1972) are in reasonably good agreement (10% or better) with a variety of more recent data, particulary those of the groups headed by Simon and by Heath (c.f. Nicolet, 1981; Simon, 1981) and from 2550 to 2900 Å they are in good agreement with the results of Mount and Rottman (1981). In this region, the results of Broadfoot are the highest of the various sets of data but still in adequate agreement. The choice between these sources seems arbitrary in this spectral range and we have adopted the results of Broadfoot. We use only Broadfoot's Table 2, which contains averages over 10 Å intervals, because his instrumental resolution was approximately 3 Å and his wavelength scale also has uncertainties of 1 Å or more. Use of his Table 1 with data at 1 Å intervals would therefore require detailed knowledge of his instrumental line shape whereas the 10 Å data can be considered (with 1% accuracy) to have a rectangular line shape. Since the data of Broadfoot were taken near aphelion, they should be increased by 3% to reduce them to 1 AU, but we have omitted this correction on the grounds that Broadfoot's data are systematically the highest of these sources by a comparable percentage.

Shortward of 2500 Å, there are serious discrepancies between the data of Broadfoot, whose data are systematically highest, and a variety of other sources. The data of Mount et al. (1980) are the lowest of the several investigators and their values are roughly 2/3 of those of Broadfoot. Mount et al. suggest that the discrepancy is due to scattered light in Broadfoot's instrument, but if this were the case one might expect the size of the discrepancy to be anticorrellated with the brightness and this is not the case. The data from Heath and from Simon lie between those of Broadfoot and those of Mount et al. (c.f. Nicolet, 1981, figs. 10a, 10b; Simon 1981, fig. 9) but significantly closer to those of Broadfoot. We therefore ignore the

results of Mount et al. The selection among the other three is more difficult. The results of Simon et al. (1982) might be questioned because they were made at relatively low altitude (41 km) and therefore required significant corrections for residual atmospheric absorption. They agree well, however, with Heath's data taken from the Nimbus satellite (c.f., Simon et al., fig. 2) indicating that these atmospheric corrections were properly applied. We conclude that in this spectral range, the data of Simon et al. (1982) are as good as any and we use their average of the two most recent measurements (their Table 2b).

We have now selected three sources of data for the absolute calibration: Simon et al. (1982; Table 2b) for $\lambda < 2410$ Å; Broadfoot (1972; Table 2) for the range $\lambda 2400 - 3200$ Å; Neckel and Labs (1981; Tables 2 and 3) for the range $\lambda 3300 - 7000$ Å. It is still necessary to combine these data in such a way as to eliminate a discontinuity at 2410 Å and to interpolate between 3200 and 3300 Å. For the bandpass $\lambda 2353 - 2381$ Å, the value of Simon et al. is .83 that of Broadfoot with no obvious trends in the ratio at shorter wavelengths. To smoothly join with Broadfoot's data, we use Broadfoot's data for the bands centered at 2390 through 2500 Å and multiply each by a value which increases linearly from .83 at 2376 Å to 1.00 at 2500 Å. Above that point, we take the values of Broadfoot and below $\lambda 2390$ we take the values of Simon et al. The results of this splicing are given in Table 1 where we give both the method of combining the sources and the actual values of the result.

For the interpolation between Broadfoot's results shortward of 3200 Å and those of Neckel and Labs longward of 3300 Å, we use the results of Simon (1975, Table 1). These results are almost equal to those of Broadfoot shortward of 3000 Å and about 10% higher than those of Neckel and Labs at 3300 Å.

Since the data of Broadfoot seem to show a systematic drop from 3000 Å to 3200 Å but have much higher spectral resolution than those of Simon, we have adopted a weighted average, as for the splicing at shorter wavelengths, with the weights varying linearly from 100% Broadfoot/0% Simon at 3000 Å to 0% Broadfoot/100% Simon at 3200 Å. We have then expressed this as a fraction of Broadfoot's data which can then be interpolated with the results given in Table 1. Similarly, we have used a weighting of 100% Simon/0% Neckel-Labs at 3250 Å linearly varying to 0% Simon/100% Neckel-Labs at 3400 Å.

The complete solar spectrum used for the calibration is given in Table 1. Although some of the calibration was done in units of energy per time per wavelength, the ultimate atlas (for our own convenience) has been converted to radiation densities at 1 AU. These are the data given in Table 1 in units of $10^{-24}$ erg $cm^{-3}$ $Hz^{-1}$ where the conversion of units was done using $\lambda$ at the center of the bandpass. The two wavelengths indicate the range over which the original flux was integrated or averaged as determined from the original reference. For all radiation densities greater than 4000 x $10^{-24}$ ergs $cm^{-3}$ $Hz^{-1}$, the numbers have been rounded to end in 0. The results are also summarized graphically in Figure 1a where we have shown the complete adopted calibration. Figure 1b shows, at expanded scales, the short-wavelength portion of the calibration which includes all overlap regions. In overlap regions, both original sources are shown as well as the adopted calibration.

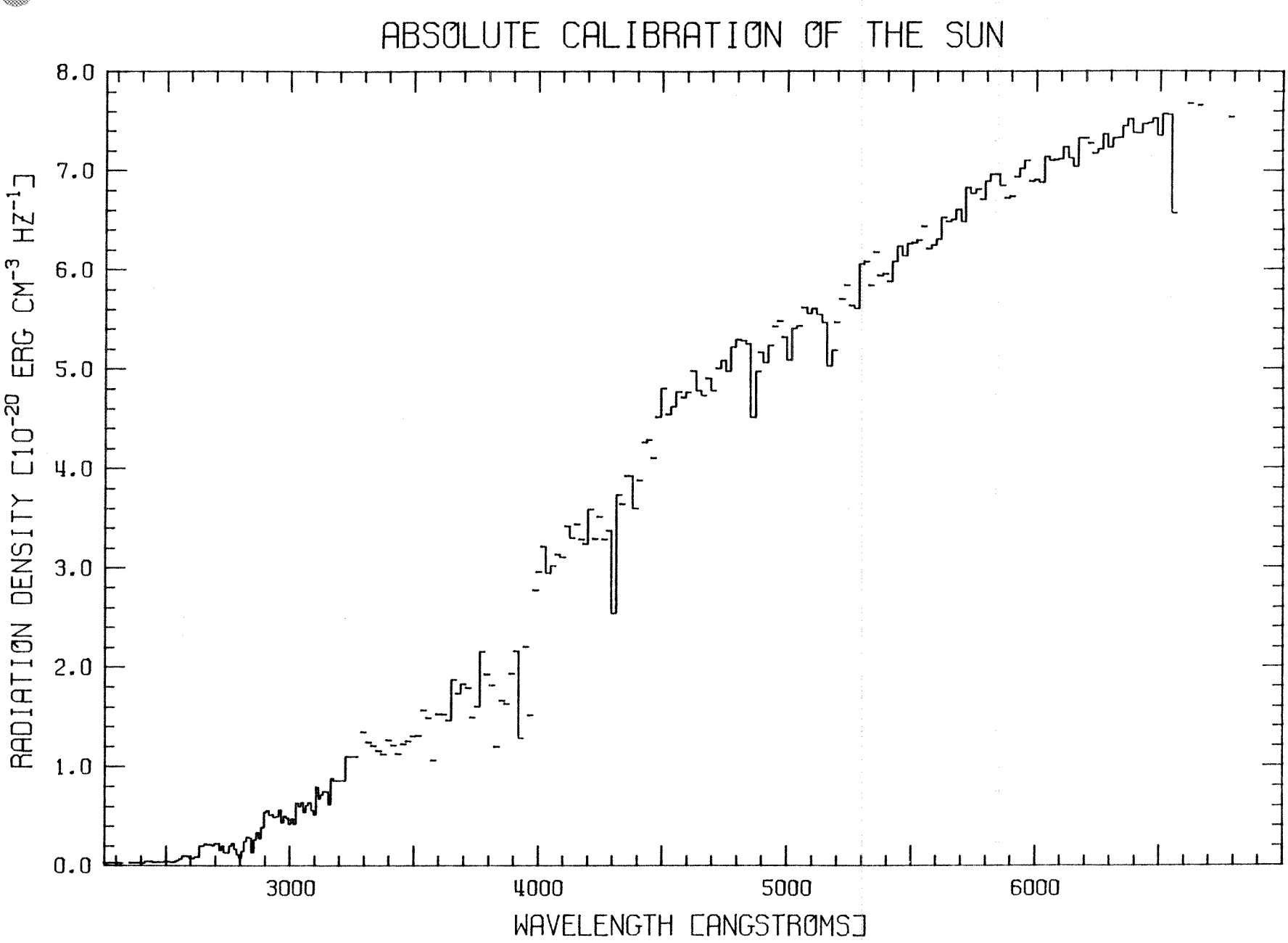


Figure 1A: The adopted, absolute calibration of the solar spectrum, also listed in Table 1. Horizontal lines indicate widths of bandpasses. Vertical lines are absent if there is either a gap or an overlap between the adjacent band passes.

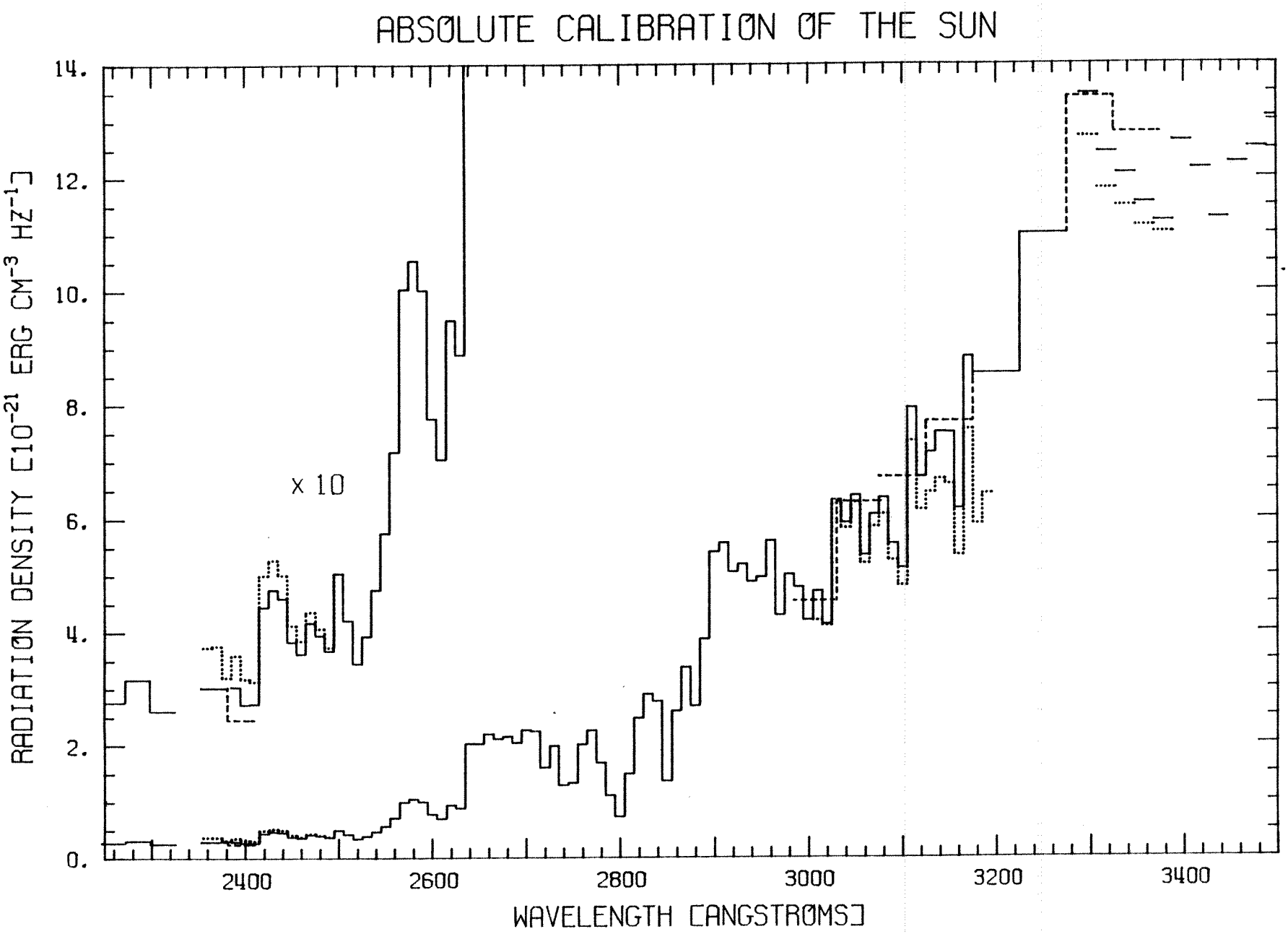


Figure 13: The solid lines again indicate the adopted calibration. Both original sources are also shown in overlap regions, using broken lines for Simon, Pastiels, and Nevejans (1982) and for Simon (1975), and dotted lines for Broadfoot (1972) and for Neckel and Labs (1981). The region shortward of 2640Å has been enlarged by a factor of 10 for clarity.

## V. THE COMBINED ATLAS

Each of the three high resolution atlases (and each piece of the KPNO atlas) was independently placed on our absolute scale before they were combined into a single atlas. The atlas was integrated over each bandpass of the absolute calibration, Table 1, and divided into the calibration value (already in units of radiation density at r = 1 AU). Each quotient was associated with the wavelength at the center of the corresponding bandpass and the set of quotients defined the calibration curve for the high resolution spectrum. These points were then fitted with a cubic spline to define a continuous calibration function and were multiplied by the high resolution atlas to provide a final absolutely calibrated atlas. The response curves are shown in Figure 2.

To combine the three atlases, we first checked for wavelength shifts between them by calculating the cross-correlation function between each pair of absolutely calibrated, high resolution spectra for all 5 Å intervals in the overlap region between the spectra. These cross-correlation functions are shown in Figure 3 and indicate both that there are wavelength shifts of order 10 mÅ between the spectra and that there is noise in the wavelength scales of order 5 mÅ. An average of the offsets shown in Figure 3 yields $\lambda_{KPNO} - \lambda_{KPK} = -0.0206 \pm .0045$ Å (rms) and $\lambda_{KPNO} - \lambda_{SP} = -0.0119 \pm .0013$ Å (rms). Note that the variations in the cross-correlation functions are much greater for KPNO vs. KPK than for KPNO vs. Sac Peak. This is consistent with the wavelength errors quoted by KPK. A comparison with laboratory wavelengths in the overlap region of Kitt Peak and Sac Peak indicated that the Sac Peak wavelength calibration was better. Therefore, we shifted the Kitt Peak spectrum redward by 0.01 Å (exactly 2 data points). This procedure is not correct since the wavelength scale of an FTS spectrum will be in error by only a multiplicative

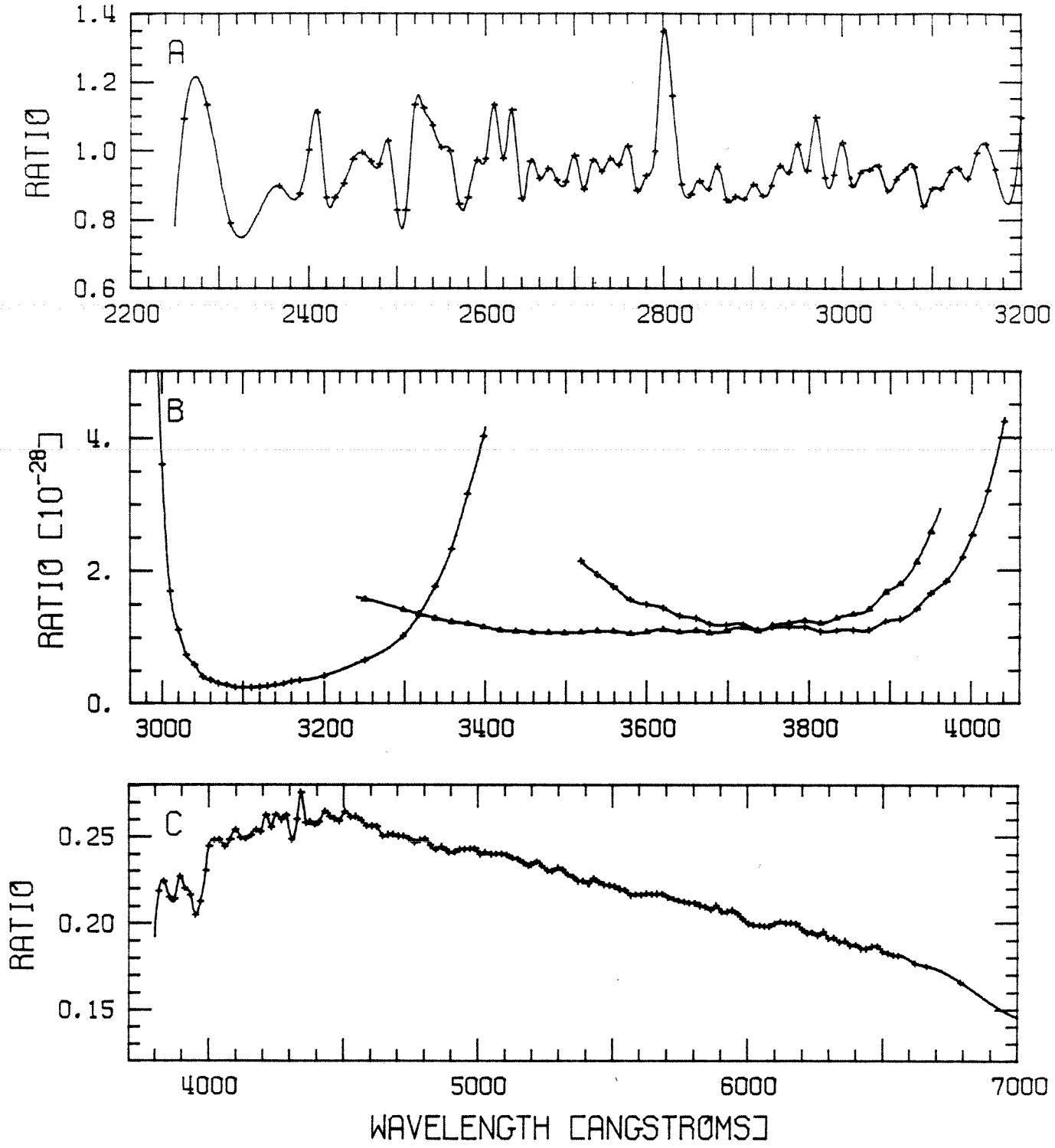


Figure 2: Response curves used for the absolute calibration of (A) the KPK atlas, (B) the Kitt Peak atlas (three individual scans), and (C) the Sac Peak atlas. Data points are the ratio between the absolute calibrations at the center of a band pass and the high resolution atlas integrated over this same band pass. A cubic spline fitted through these data points yields the continuous calibration function. The scale for the ordinate in (B) has an unusual exponent because the Kitt Peak scans had no previous calibration applied to them. The largest deviations from a smooth curve are all associated with strong, solar absorption features.

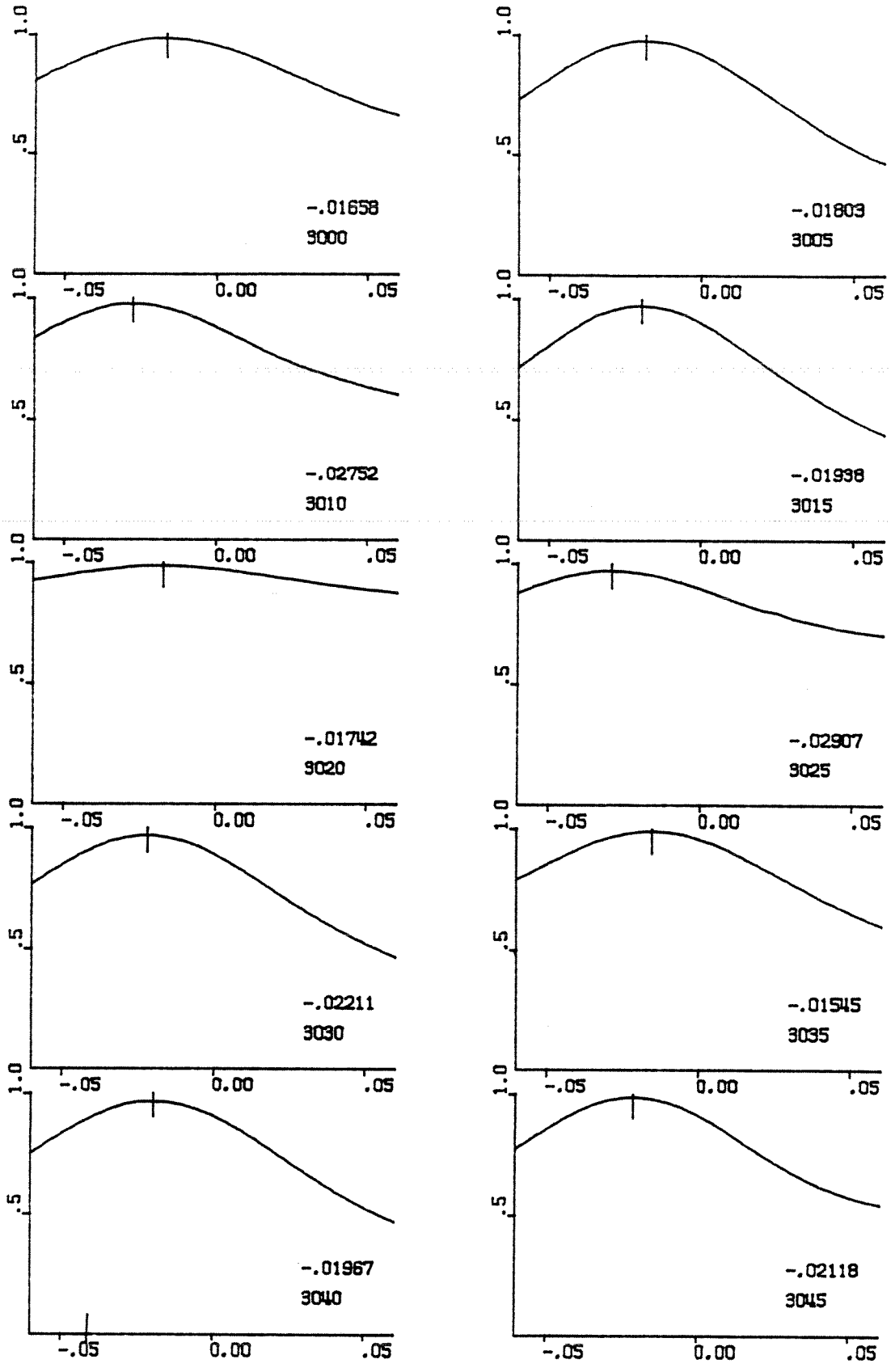


Figure 3A: Cross-correlation between Kitt Peak and KPK atlases for each 5Å interval in the overlapping region. The peaks, indicated by the vertical tic marks, show the wavelength offset between the two atlases. Each panel is labelled by the offset and by the shortest wavelength in the 5Å interval. Average offset is -0.0206Å with 0.0045Å (rms) fluctuation.

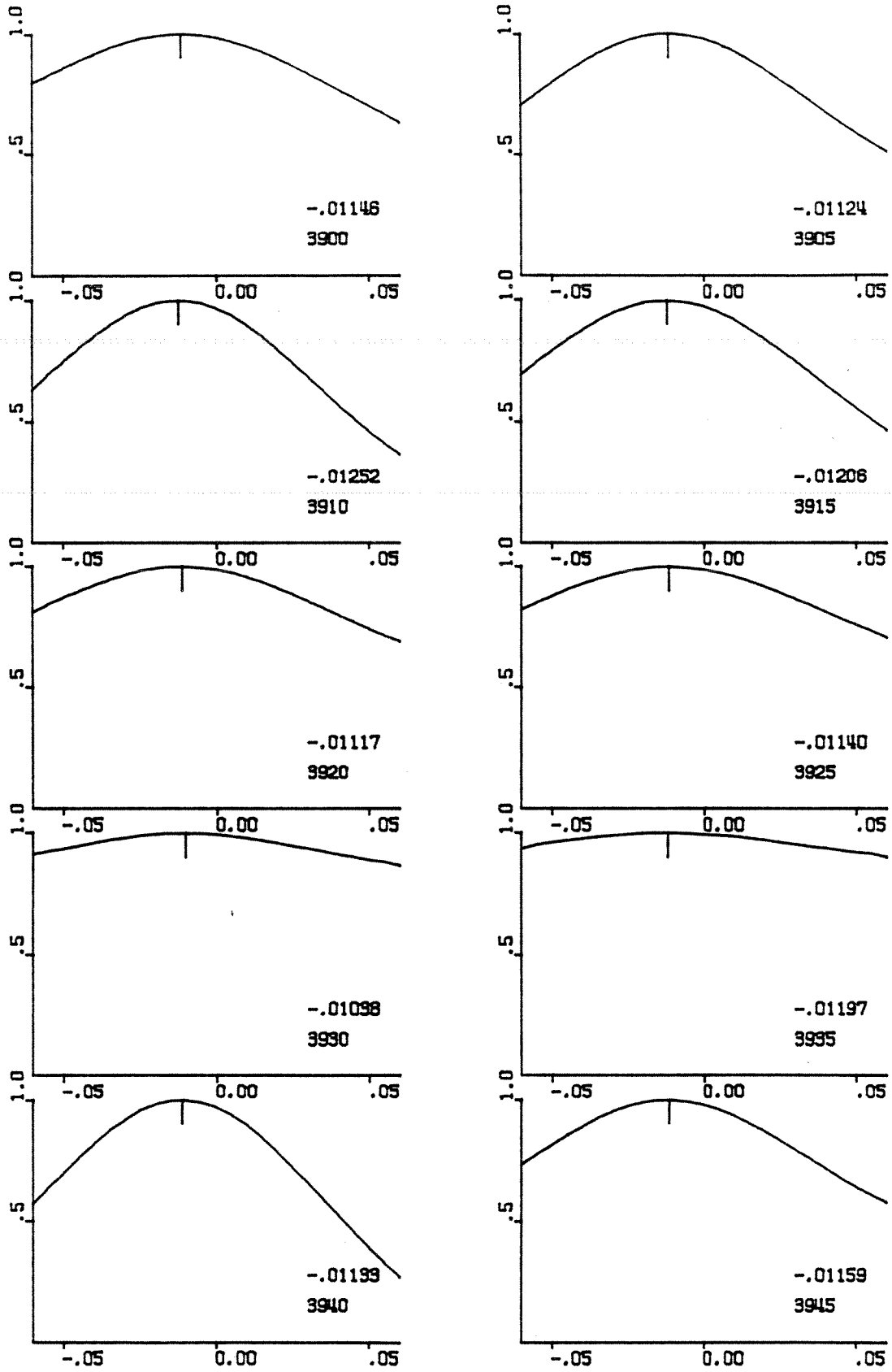


Figure 3B: Cross-correlation between KPNO and Sac Peak atlases for each 5Å interval in the overlapping region. The peaks, indicated by the vertical tic marks, show the wavelength offset between the two atlases. Each panel is labelled by the offset and by the shortest wavelength in the 5Å interval. Average offset is -0.0119Å with 0.0013Å (rms) variation.

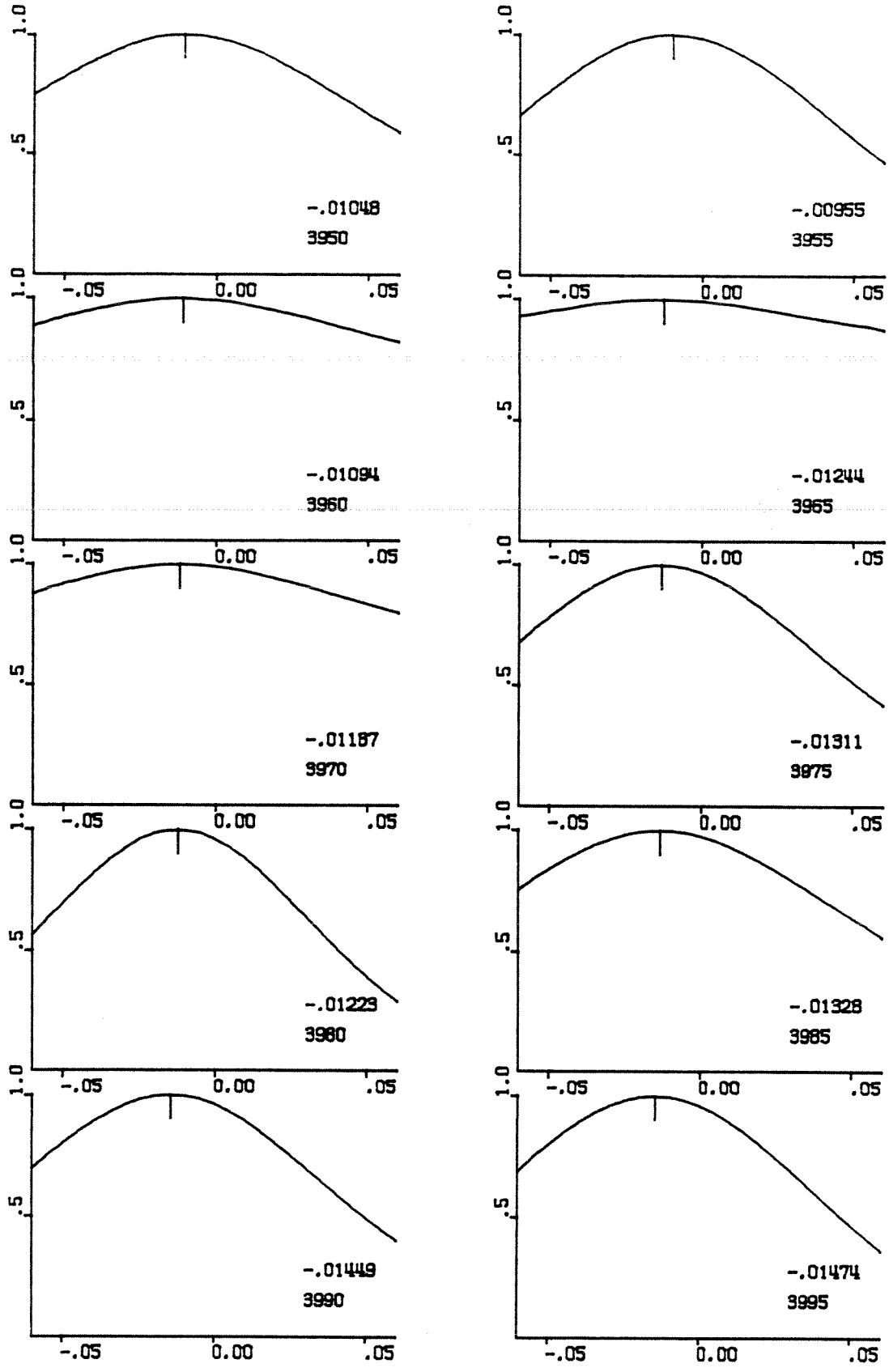


Figure 3B -- continued.

factor, but as the difference in the shift between 3000 and 4000 Å would be significantly smaller than our desired resolution we opted for the simpler approach of a constant shift. To bring the KPK atlas into agreement both with the KPNO atlas and with laboratory wavelengths over the range 3000 to 3050 Å, we shifted the KPK atlas blueward by 0.01 Å.

Finally, we used a linearly varying weighting function to merge the three atlases in their overlap regions. The weighting functions used varied from 100% KPK/0% KPNO at 3000 Å to 0% KPK/100% KPNO at 3050 Å and from 100% KPNO/0% Sac Peak at 3900 Å to 0% KPNO/100% Sac Peak at 4000 Å.

In Figure 4 we show portions of the overlap regions of the final spectra, showing both original sources after application of the wavelength shifts described above. Note that even over the scale of a few Angstroms there is significant jitter in wavelength when KPK and KPNO are compared; when KPNO and Sac Peak are compared, the jitter in wavelength is less than our wavelength spacing of 5 mÅ. This suggests that the final atlas may have wavelength uncertainties significantly greater than the spacing, perhaps up to 10 or 20 mÅ, for wavelengths less than 3050 Å but not for longer wavelengths.

We will point out only one comparison of our atlas with others. Donn, Cody, Kumar, and Wiant (private communication) have utilized a precedure similar to ours but with totally independent data to obtain a corresponding atlas. Their high resolution spectrum was obtained at Kitt Peak by Kumar and they used the absolute solar irradiance of Mount and Rottman (1981). Thus far they have calibrated only a portion of their atlas, viz the region from 3000 to 3200 Å. Wiant has carried out a point by point comparison between our two atlases for the few Angstroms in the vicinity of the strongest OH absorption. He finds excellent agreement between the two atlases with the largest differences amounting to approximately 10% of the continuum.

## IV. HIGH RESOLUTION SPECTRA

As with the data for absolute calibration, it has been necessary to obtain the high resolution data from several sources in order to cover the desired wavelength range. Since line strengths and shapes vary from the center of the solar disc to the limb, it is necessary to have high resolution data which refer to the whole disc. This drastically limits the number of available sources of data. As noted above, we require for our purposes a spectral resolution of order 1 km/sec (10 mÅ at 3000 Å) and a corresponding accuracy for the wavelength scale.

### A. λ3800 - 7000 Å

For most of the optical range we have adopted the atlas of Beckers et al. (1976) taken at Sacramento Peak Observatory (Sac Peak hereafter). This spectrum was obtained by using a cylindrical lens of only 5 mm focal length to image the sun onto the entrance slit of a double-pass spectrometer. The spectrometer was used with two different gratings in 8th to 15th orders with 100 Å interference filters to isolate the order of interest. The data (in the magnetic tape version of the atlas) are sampled at 5 mÅ intervals. The resolving power was approximately 300,000 for the range from λ4000 - 7000 Å (13 mÅ at 4000 Å ~ 1 km/sec) and 192,000 for the range λ3800 - 4000 Å (21 mÅ at 4000 Å, ~ 1.5 km/sec). To reduce noise, the data were additionally smoothed with a Gaussian filter of width at the $e^{-1}$ point $\pm \lambda/750,000$ (10 mÅ at 4000 Å). As noted in the introduction to that atlas, there should be no fine structure at higher resolution than this because of solar rotation.

The original atlas was normalized to a continuum intensity of 0.9, but because they carried out the scans in small sections (10 - 20 Å each) there

may be errors of several percent in defining the continuum level near strong Fraunhofer lines.

Because many of our calculations involve wavelengths deduced from molecular constants and because we are combining both optical and ultraviolet data, it was decided to use all wavelengths in vacuum. Since the Sac Peak Atlas uses wavelengths in air, it was necessary to convert the wavelength scale. For equally spaced values of $\lambda_{vac}$ we calculated $\lambda_{air}$ from

$$\lambda_{vac}/\lambda_{air} = 1 + 10^{-6}\{64.328 + 29498.1/[146 - 1/\lambda_v^2] + 255.4/[41-1/\lambda_v^2]\} \quad (1)$$

using $\lambda$ in microns (c.f., Allen 1973, p. 124). The flux from the Sac Peak Atlas was interpolated to this wavelength in air.

B. $\lambda$3000 - 4050 Å

Data for this spectral range were obtained by R. A. West at Kitt Peak National Observatory using the Fourier Transform Spectrometer (FTS) at the McMath Solar Telescope. This instrument provides full-disc spectra at high spectral resolution. The three original interferograms were taken on 21 and 22 June 1981 with the sun near transit to minimize losses due to the severe atmospheric attenuation at these wavelengths. They cover three separate but overlapping spectral regions to produce spectra covering the regions: a. (2887 - 3435 Å), b. (3233 - 3977 Å) and c. (3487 - 4057 Å). The maximum airmasses were 1.05, 1.21, and 1.30 for a, b, and c, respectively. Because of the filters used to prevent aliasing in the interferograms, the signal dropped essentially to zero near the ends of these spectral ranges and the full range

is not useful. Each interferogram consisted of ~ 7 x $10^5$ points yielding a resolving power near 3.5 x $10^5$ or a resolution near 10 mÅ.

The spectra, as obtained on magnetic tape from G. Ladd at Kitt Peak, were interpolated to 0.005 Å intervals (vacuum wavelengths) and the overlap regions plotted to check for consistency. The agreement in the overlap regions was excellent so the spectra were merged, after applying the absolute calibration, into a single spectrum using a linear weighted average in the overlap regions. In other words, between 3240 and 3400 Å , the weighting varied linearly from 100% spectrum a/0% spectrum b at 3240 Å to 0% spectrum a/100% spectrum b at 3400 Å and similarly between 3520 and 3960 Å for spectra b and c.

No attempt was made to explicitly correct for atmospheric attenuation. Attentuation varying slowly with wavelength is automatically removed during the application of the absolute calibration. Discrete absorption features, e.g., due to telluric $O_3$, may still remain. Because of our interest in OH, the spectral region from 3070 to 3085 Å was carefully compared with the spectrum of the center of the disc measured with a rocket by Kohl, Parkinson, and Kurucz (1978). No discrete telluric features could be identified in this region. However, features of significant strength may exist in other wavelength regions.

C. λ2250 - 3050 Å

For this spectral region we have utilized the atlas of Kohl, Parkinson, and Kurucz (1978, KPK hereafter). This atlas contains spectra of the center of the disc and of a position near the limb ($\mu$ = 0.23). The spectral resolution is 0.028 Å, slightly coarse for our needs but still the most appropriate data available. In addition, the wavelength scale itself is accurate only to about 0.02 Å, another significant limitation from our point

of view. The magnetic tape version of the atlas is tabulated, however, at 5 mÅ intervals of wavelength in air.

Kohl et al. (1980) have used the KPK atlas to derive total solar irradiance by assuming a shape for the limb darkening curve and assuming that the spectrum for the center of the disk is valid for the interval $1.0 > \mu > 0.23$ and that the spectrum for the limb is valid over the interval from $0.23 > \mu \geq 0.0$. Since we are applying a separate absolute calibration, we need only the relative weights of the two spectra but in earlier work we did try to maintain the absolute intensity calibration of the KPK atlas. Using the limb-darkening coefficients of Allen (1973, p. 171) we deduced the weighting

$$I_\lambda = 0.545\, I_{\mu=1} + \begin{cases} 0.330\, I_{\mu=0.23} \\ 0.080\, I_{\mu=1} \quad (\text{if } I_{\mu=0.23} \text{ is not given}) \end{cases} \qquad (2)$$

The second form is needed over selected wavelength intervals in which KPK do not give a spectrum for the limb. Most of these regions are at the longer wavelengths and it is for this reason that we have discarded all data from KPK for $\lambda > 3050$ Å.

The comparison of the solar spectral irradiance deduced from this atlas with many other sources has been discussed in some detail by Kohl et al. (1980) and will not be repeated here. The atlas wavelengths were converted from air to vacuum and interpolated to uniform 5 mÅ intervals in vacuum wavelength.

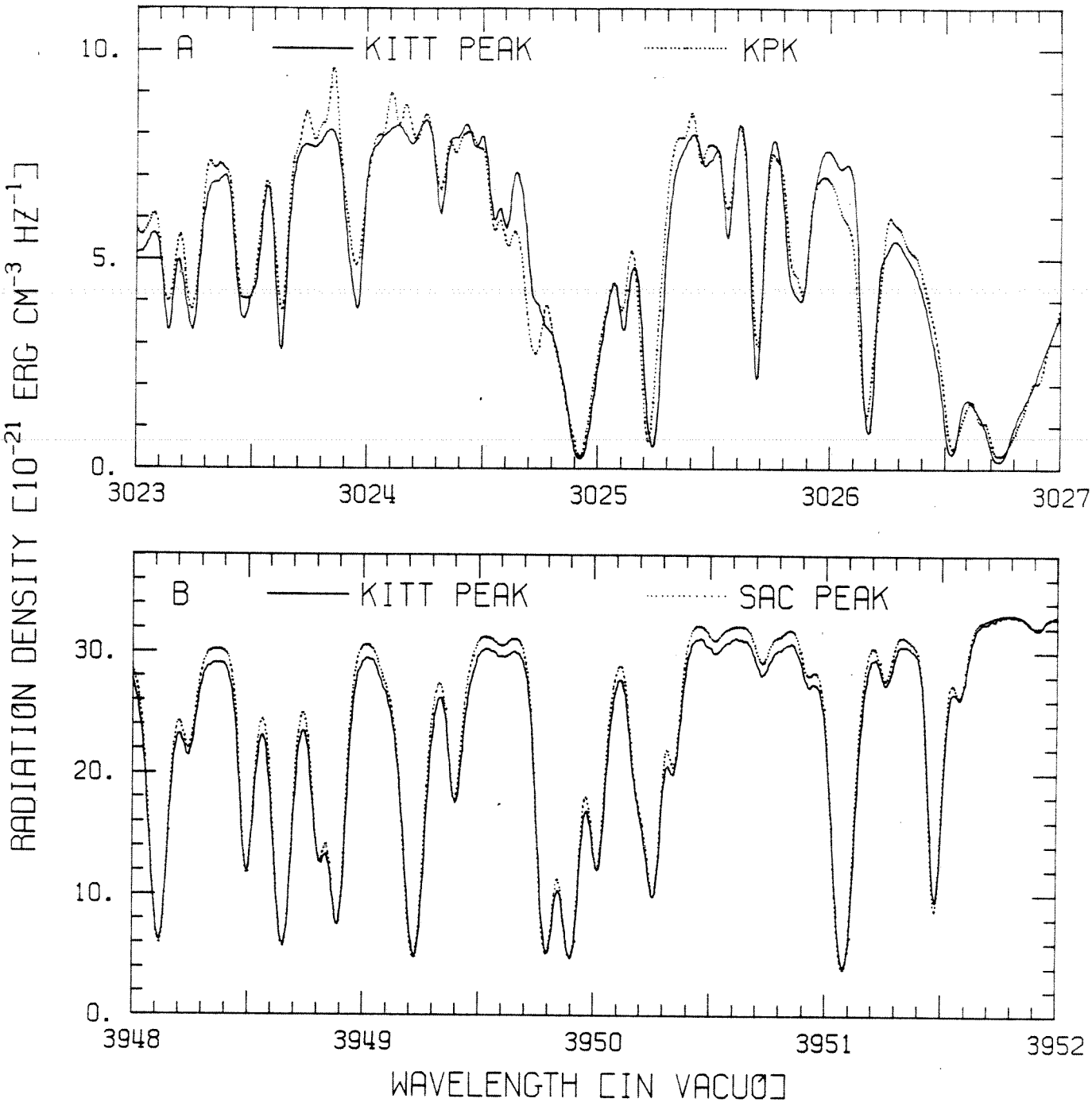


Figure 4: The middle of the overlap region of (A) Kitt Peak (solid) and KPK (dotted) atlases and of (B) Kitt Peak (solid) and Sac Peak (dotted) atlases after absolute calibration and application of the wavelength shifts described in the text.

This portion of our spectrum is shown in Figure 5 where we have superimposed the positions of the five absorption transitions which dominate the ultraviolet pumping of OH. For comparison purposes, we also show a spectrum based solely on the center-of-disc spectrum of KPK which we used in a previous study of OH fluorescence (Schleicher and A'Hearn, 1982). The differences are significant and are due to several factors including the change from center-of-disc to whole disc, the systematic shift in wavelength, the reduced jitter in wavelength of the KPNO data, and the new absolute calibration.

We conclude that our atlas can be used for calculations of fluorescent spectra with confidence. The uncertanties in the solar flux should generally not be the limiting factors in the accuracy of the resultant spectra although the wavelength errors shortward of 3050 Å may lead to errors in deduced fluxes greater than 10%.

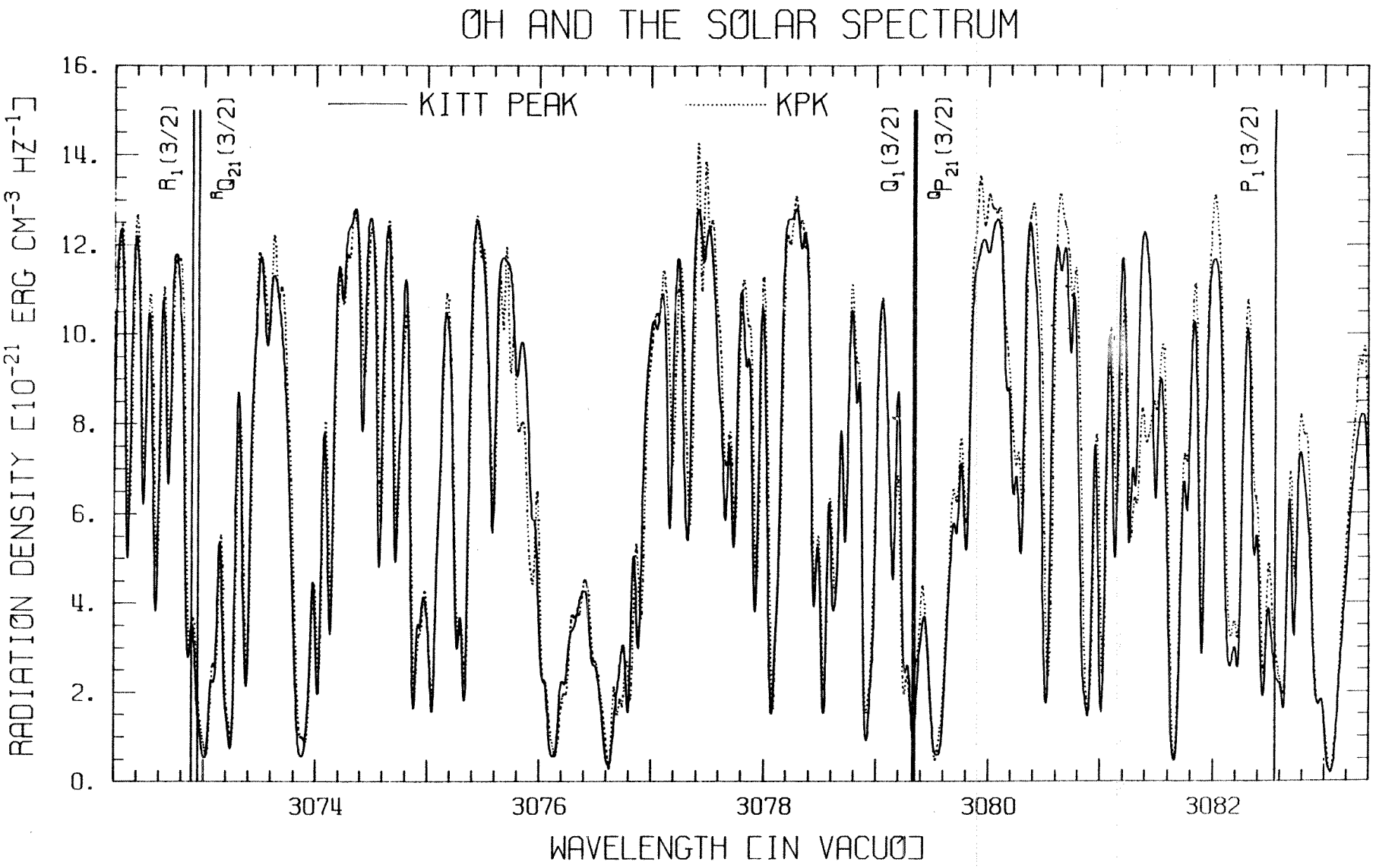


Figure 5: The major lines of the $A^2\Sigma^+ - X^2\Pi$ 0-0 band of OH arising from the ground state - which dominate the fluorescence process in cometary OH - are overlaid on our adopted solar spectrum (solid) and on the original KPK atlas, used in our previous OH fluorescence calculation (Schleicher and A'Hearn 1982). The KPK atlas shown has been shifted from air to vacuum wavelengths and converted to units of radiation density at 1 AU. Line positions are for zero Doppler shift; a change of heliocentric radial velocity of 10 km $s^{-1}$ corresponds to approximately a 0.1Å shift.

## VI. AVAILABILITY

The final magnetic tape version of the atlas is available from the authors. Our own tape is 9-track, written in UNIVAC 1180 binary format. We will also provide tapes written in ASCII upon request. The data are blocked in records of 1002 words each, with the first two words being the number of data points in the record (always 1000) and the wavelength in Angstroms of the first point. The remaining 1000 words are the radiation densities at 1 AU (erg $cm^{-3}$ $Hz^{-1}$) at intervals of 0.005 Å. Thus each record covers 5 Å. A graphical version of the portion of the atlas covering λ2250 - 4000 Å will also be available. The portion of the atlas longward of 4000 Å is not available from us in graphical form, since it differs from the previously published atlas (Beckers et al. 1976) only by a wavelength shift (air to vacuum) and the smoothly varying response curve of Figure 2. Potential users needing either the magnetic tape or the graphical display should contact the authors to make arrangements for reproduction of copies.

## VII. ACKNOWLEDGEMENTS

We thank R. A. West who originally obtained the FTS spectra at Kitt Peak and brought its existence to our attention and we also thank G. Ladd and J. Brault of Kitt Peak for providing details about these spectra. We had helpful discussions with B. Donn, R. Cody and M. Wiant regarding the difficulties encountered in producing an atlas such as this and we thank M. Wiant for providing the comparison between our results. D. Messina assisted with programming the absolute calibration of the Sac Peak atlas and its conversion from air to vacuum wavelengths. Computer time was provided by the University of Maryland Computer Science Center. Some financial support was also provided by NASA grants NSG 7322 and NAG 5-274 to the University of Maryland.

# REFERENCES

Allen. C.W., (1973). "Astrophysical Quantities," 3rd edition, (London: Athlone Press).

Beckers, Jacques M., Charles, A. Bridges, and Lou B. Gillian (1976). "A High Resolution Spectral Atlas of the Solar Irradiance from 380 to 700 Nanometers." Air Force Geophysical Laboratory Publication, AFGL-TR-76-0126.

Broadfoot, A. Lyle (1972). "The Solar Spectrum 2100 - 3200 Å." Ap. J., 173, 681-689.

Fröhlich, Claus (1981). "The Variability of the Solar Output." in Variations of the Solar Constant, ed., S. Sofia (NASA CP-2191, U.S. Govt. Print. Off.) pp. 37-44.

Hardorp, Johannes (1980). "The Sun Among the Stars. III. Energy Distribution of 16 Northern G-Type Stars and the Solar Flux Calibration." Astron. Astrophys., 91, 221-232.

Kohl, John L., William H. Parkinson, and Robert L. Kurucz (1978). "Center and Limb Solar Spectrum in High Spectral Resolution 225.2 nm to 319.6 nm." (Cambridge: Harvard-Smithsonian Center for Astrophysics) QB541 .K62

Kohl, John L., William H. Parkinson, and Carlos A. Zapata (1980). "Solar Spectral Radiance and Irradiance at 225.2 - 319.6 Nanometers", Ap. J. Suppl. Ser., 44, 295-317.

Labs, Dietrich and Heinz Neckel (1968). "The Radiation of the Solar Photosphere from 2000 Å to 100 μ." Zs. f. Ap., 69, 1-73.

Livingston, W., H. Holweger, and O.R. White (1981). "Observed Variability in the Fraunhofer Line Spectrum of Solar Flux, 1975 - 1980." in Variations of the Solar Constant., ed. S. Sofia (NASA CP-2191, U.S. Govt. Print. Off.) pp. 95-109.

Mount, George H. and Gary J Rottman (1981). "The Solar Spectral Irradiance 1200 - 3184 Å Near Solar Maximum: July 15, 1980." J.G.R., 86, 9193-9198.

Mount, George H., Gary J. Rottman, and J. Gethyn Timothy (1980). "The Solar Spectral Irradiance 1200 - 2550 Å at Solar Maximum." J.G.R., 85, 4271 - 4274.

Neckel, Heinz and Dietrich Labs (1981). "Improved Data of Solar Spectral Irradiance from 0.33 to 1.25 μ." Solar Phys., 74, 231-249.

Nicolet, Marcel (1981). "The Solar Spectral Irradiance and its Action in the Atmospheric Photodissociation Process." Planet. Space Sci., 29, 951-974.

Schleicher, David G. and Michael F. A'Hearn (1981). "OH Fluorescence in Comets: Fluorescence Efficiency of the Ultraviolet Bands." Ap. J., 258, 864-877.

Simon, P. (1975). "Nouvelles mesures de l'ultraviolet solaire dans la stratosphère." Bull. Acad. Roy. Belg. (Class. Sci.), 61, 399-409.

Simon, Paul C. (1981). "Solar Irradiance Between 120 and 400 nm and its Variations." Solar Physics, 74, 273-291.

Simon, Paul C., Roger Pastiels, and Dennis Nevejans (1982). "Balloon Observations of Solar Ultraviolet Irradiance at Solar Minimum." Plan. Space Sci., 30, 67-71.

Smith, Elske v.P. and David M. Gotlieb (1974). "Solar Flux and Its Variations." Space Sci. Rev., 16, 771-802.

SOLUMD



Table 1: Adopted Absolute Calibration of the Sun at Low Resolution

| $\lambda_1$ [Å] | $\lambda_2$ [Å] | $\rho_\nu$ [$10^{-24}$ergcm$^{-3}$Hz$^{-1}$] | Source[1] |
|---|---|---|---|
| 2247.2 | 2272.7 | 277 | SPN |
| 2272.7 | 2298.9 | 317 | SPN |
| 2298.9 | 2325.5 | 261 | SPN |
| 2352.9 | 2381.0 | 302 | SPN = .830B |
| 2385.0 | 2395.0 | 304 | .847B |
| 2395.0 | 2405.0 | 273 | .861B |
| 2405.0 | 2415.0 | 274 | .875B |
| 2415.0 | 2425.0 | 445 | .888B |
| 2425.0 | 2435.0 | 476 | .902B |
| 2435.0 | 2445.0 | 460 | .916B |
| 2445.0 | 2455.0 | 383 | .930B |
| 2455.0 | 2465.0 | 362 | .943B |
| 2465.0 | 2475.0 | 417 | .957B |
| 2475.0 | 2485.0 | 394 | .971B |
| 2485.0 | 2495.0 | 367 | .985B |
| 2495.0 | 2505.0 | 504 | B |
| 2505.0 | 2515.0 | 420 | B |
| 2515.0 | 2525.0 | 344 | B |
| 2525.0 | 2535.0 | 393 | B |
| 2535.0 | 2545.0 | 475 | B |
| 2545.0 | 2555.0 | 575 | B |
| 2555.0 | 2565.0 | 718 | B |
| 2565.0 | 2575.0 | 1005 | B |
| 2575.0 | 2585.0 | 1055 | B |
| 2585.0 | 2595.0 | 1002 | B |
| 2595.0 | 2605.0 | 776 | B |
| 2605.0 | 2615.0 | 704 | B |
| 2615.0 | 2625.0 | 950 | B |
| 2625.0 | 2635.0 | 889 | B |
| 2635.0 | 2645.0 | 2036 | B |
| 2645.0 | 2655.0 | 2026 | B |
| 2655.0 | 2665.0 | 2199 | B |
| 2665.0 | 2675.0 | 2112 | B |
| 2675.0 | 2685.0 | 2156 | B |
| 2685.0 | 2695.0 | 2039 | B |
| 2695.0 | 2705.0 | 2268 | B |
| 2705.0 | 2715.0 | 2246 | B |

| | | | |
|---|---|---|---|
| 2715.0 | 2725.0 | 1605 | B |
| 2725.0 | 2735.0 | 1991 | B |
| 2735.0 | 2745.0 | 1284 | B |
| 2745.0 | 2755.0 | 1337 | B |
| 2755.0 | 2765.0 | 2013 | B |
| 2765.0 | 2775.0 | 2259 | B |
| 2775.0 | 2785.0 | 1683 | B |
| 2785.0 | 2795.0 | 1104 | B |
| 2795.0 | 2805.0 | 737 | B |
| 2805.0 | 2815.0 | 1490 | B |
| 2815.0 | 2825.0 | 2480 $\times 10^{-24}$ erg/cm$^3$ Hz | B |
| 2825.0 | 2835.0 | 2902 | B |
| 2835.0 | 2845.0 | 2768 | B |
| 2845.0 | 2855.0 | 1354 | B |
| 2855.0 | 2865.0 | 2604 | B |
| 2865.0 | 2875.0 | 3374 | B |
| 2875.0 | 2885.0 | 2692 | B |
| 2885.0 | 2895.0 | 3870 | B |
| 2895.0 | 2905.0 | 5420 | B |
| 2905.0 | 2915.0 | 5580 | B |
| 2915.0 | 2925.0 | 5060 | B |
| 2925.0 | 2935.0 | 5200 | B |
| 2935.0 | 2945.0 | 4890 | B |
| 2945.0 | 2955.0 | 4980 | B |
| 2955.0 | 2965.0 | 5610 | B |
| 2965.0 | 2975.0 | 4290 | B |
| 2975.0 | 2985.0 | 5020 | B |
| 2985.0 | 2995.0 | 4790 | B |
| 2995.0 | 3005.0 | 4210 | B |
| 3005.0 | 3015.0 | 4720 | 1.004B |
| 3015.0 | 3025.0 | 4140 | 1.008B |
| 3025.0 | 3035.0 | 6330 | 1.012B |
| 3035.0 | 3045.0 | 5930 | 1.016B |
| 3045.0 | 3055.0 | 6410 | 1.020B = .075B + 0.25S |
| 3055.0 | 3065.0 | 5360 | 1.029B |
| 3065.0 | 3075.0 | 6080 | 1.038B |
| 3075.0 | 3085.0 | 6360 | 1.047B |
| 3085.0 | 3095.0 | 5560 | 1.056B |
| 3095.0 | 3105.0 | 5130 | 1.065B = .0.50B + 0.50S |
| 3105.0 | 3115.0 | 7940 | 1.080B |
| 3115.0 | 3125.0 | 6730 | 1.094B |
| 3125.0 | 3135.0 | 7150 | 1.108B |
| 3135.0 | 3145.0 | 7510 | 1.123B |
| 3145.0 | 3155.0 | 7500 | 1.138B = 0.25B + 0.75S |
| 3155.0 | 3165.0 | 6170 | 1.153B |

| | | | |
|---|---|---|---|
| 3165.0 | 3175.0 | 8840 | 1.168B |
| 3175.0 | 3225.0 | 8540 | S |
| 3225.0 | 3275.0 | 11010 | S |
| 3287.9 | 3308.4 | 13470 | 1.060NL = 0.33NL + 0.67S |
| 3307.4 | 3327.9 | 12440 | 1.055NL |
| 3327.7 | 3348.2 | 12070 | 1.051NL = 0.59NL + 0.41S |
| 3348.3 | 3368.8 | 11550 | 1.037NL |
| 3368.4 | 3388.9 | 11220 | 1.018NL |
| 3388.0 | 3408.5 | 12640 | NL |
| 3408.4 | 3428.9 | 12150 | NL |
| 3427.7 | 3448.2 | 11270 | NL |
| 3448.0 | 3468.5 | 12260 | NL |
| 3468.3 | 3488.8 | 12530 | NL |
| 3487.9 | 3508.4 | 13070 | NL |
| 3508.3 | 3528.8 | 13080 | NL |
| 3528.7 | 2549.2 | 15700 | NL |
| 3548.8 | 3569.3 | 14850 | NL |
| 3569.1 | 3589.6 | 10610 | NL |
| 3589.3 | 3609.8 | 15310 | NL |
| 3609.9 | 3630.4 | 15210 | NL |
| 3630.3 | 3650.8 | 14620 | NL |
| 3650.8 | 3671.3 | 18740 | NL |
| 3667.5 | 3688.0 | 17300 | NL |
| 3688.0 | 3708.5 | 18270 | NL |
| 3708.4 | 3728.9 | 17860 | NL |
| 3726.4 | 3746.9 | 14920 | NL |
| 3744.5 | 3765.0 | 16020 | NL |
| 3765.0 | 3785.5 | 21510 | NL |
| 3784.1 | 3804.6 | 19220 | NL |
| 3803.7 | 3824.2 | 18130 | NL |
| 3823.3 | 3843.8 | 11950 | NL |
| 3843.5 | 3864.0 | 16620 | NL |
| 3863.5 | 3884.0 | 16280 | NL |
| 3883.9 | 3904.4 | 19310 | NL |
| 3901.7 | 3922.2 | 21590 | NL |
| 3922.2 | 3942.7 | 12850 | NL |
| 3940.0 | 3960.5 | 22040 | NL |
| 3959.0 | 3979.5 | 15160 | NL |
| 3979.0 | 3999.5 | 27740 | NL |
| 3990.8 | 4011.3 | 29570 | NL |
| 4010.0 | 4030.0 | 32100 | NL |
| 4030.0 | 4050.0 | 29450 | NL |
| 4050.0 | 4070.0 | 30180 | NL |
| 4068.8 | 4088.8 | 31310 | NL |
| 4088.8 | 4108.8 | 31030 | NL |

| | | | |
|---|---|---|---|
| 4107.1 | 4127.1 | 34200 | NL |
| 4127.1 | 4147.1 | 33000 | NL |
| 4146.5 | 4166.5 | 34380 | NL |
| 4165.9 | 4185.9 | 32840 | NL |
| 4181.2 | 4201.2 | 32370 | NL |
| 4201.2 | 4221.2 | 35880 | NL |
| 4221.0 | 4241.0 | 32860 | NL |
| 4237.5 | 4257.5 | 35150 | NL |
| 4257.9 | 4277.9 | 32830 | NL |
| 4276.4 | 4296.4 | 33710 | NL |
| 4296.4 | 4316.4 | 25380 | NL |
| 4316.4 | 4336.4 | 37350 | NL |
| 4329.7 | 4349.7 | 36390 | NL |
| 4349.2 | 4369.2 | 39230 | NL |
| 4361.9 | 4381.9 | 39200 | NL |
| 4381.9 | 4401.9 | 35910 | NL |
| 4399.0 | 4419.0 | 38790 | NL |
| 4418.0 | 4438.0 | 42660 | NL |
| 4437.2 | 4457.2 | 42860 | NL |
| 4454.0 | 4474.0 | 41050 | NL |
| 4473.2 | 4493.2 | 45170 | NL |
| 4493.2 | 4513.2 | 48060 | NL |
| 4513.6 | 4533.6 | 45450 | NL |
| 4533.6 | 4553.6 | 46240 | NL |
| 4553.6 | 4573.6 | 47710 | NL |
| 4573.7 | 4593.7 | 47130 | NL |
| 4593.7 | 4613.7 | 47670 | NL |
| 4613.6 | 4633.6 | 49820 | NL |
| 4633.6 | 4653.6 | 47850 | NL |
| 4653.6 | 4673.6 | 47340 | NL |
| 4673.5 | 4693.5 | 49080 | NL |
| 4693.5 | 4713.5 | 47820 | NL |
| 4713.3 | 4733.3 | 50100 | NL |
| 4733.3 | 4753.3 | 50870 | NL |
| 4753.3 | 4773.3 | 49780 | NL |
| 4773.3 | 4793.3 | 52200 | NL |
| 4793.3 | 4813.3 | 52980 | NL |
| 4813.3 | 4833.3 | 52840 | NL |
| 4833.1 | 4853.1 | 52510 | NL |
| 4853.1 | 4873.1 | 45130 | NL |
| 4873.1 | 4893.1 | 49810 | NL |
| 4882.9 | 4902.9 | 51660 | NL |
| 4902.9 | 4922.9 | 50590 | NL |
| 4922.9 | 4942.9 | 52390 | NL |
| 4941.5 | 4961.5 | 54260 | NL |

| | | | |
|---|---|---|---|
| 4960.7 | 4980.7 | 54800 | NL |
| 4978.9 | 4998.9 | 53200 | NL |
| 4998.9 | 5018.9 | 50900 | NL |
| 5018.9 | 5038.9 | 54080 | NL |
| 5038.9 | 5058.9 | 54330 | NL |
| | | | |
| 5058.3 | 5078.3 | 56220 | NL |
| 5078.3 | 5098.3 | 55520 | NL |
| 5098.3 | 5118.3 | 56090 | NL |
| 5118.3 | 5138.3 | 55450 | NL |
| 5138.3 | 5158.3 | 54630 | NL |
| | | | |
| 5158.3 | 5178.3 | 50280 | NL |
| 5178.3 | 5198.3 | 51900 | NL |
| 5189.5 | 5209.5 | 54680 | NL |
| 5209.3 | 5229.3 | 57010 | NL |
| 5228.8 | 5248.8 | 58430 | NL |
| | | | |
| 5248.0 | 5268.0 | 56340 | NL |
| 5268.0 | 5288.0 | 56040 | NL |
| 5288.0 | 5308.0 | 60620 | NL |
| 5306.5 | 5326.5 | 60820 | NL |
| 5325.2 | 5345.2 | 58380 | NL |
| | | | |
| 5343.9 | 5363.9 | 61790 | NL |
| 5362.0 | 5382.0 | 59380 | NL |
| 5381.5 | 5401.5 | 59590 | NL |
| 5400.0 | 5420.0 | 58780 | NL |
| 5420.0 | 5440.0 | 62380 | NL |
| | | | |
| 5440.0 | 5460.0 | 60840 | NL |
| 5460.0 | 5480.0 | 61370 | NL |
| 5480.0 | 5500.0 | 62620 | NL |
| 5498.0 | 5518.0 | 62720 | NL |
| 5517.3 | 5537.3 | 63000 | NL |
| | | | |
| 5537.0 | 5557.0 | 64390 | NL |
| 5556.9 | 5576.9 | 62080 | NL |
| 5576.9 | 5596.9 | 62490 | NL |
| 5596.9 | 5616.9 | 63100 | NL |
| 5616.9 | 5636.9 | 65290 | NL |
| | | | |
| 5636.0 | 5656.0 | 64870 | NL |
| 5656.0 | 5676.0 | 65080 | NL |
| 5676.0 | 5696.0 | 66080 | NL |
| 5696.0 | 5716.0 | 64810 | NL |
| 5716.0 | 5736.0 | 68310 | NL |
| | | | |
| 5736.0 | 5756.0 | 67680 | NL |
| 5756.0 | 5776.0 | 68120 | NL |
| 5774.5 | 5794.5 | 67100 | NL |
| 5794.5 | 5814.5 | 68970 | NL |
| 5814.5 | 5834.5 | 69600 | NL |

| | | | |
|---|---|---|---|
| 5834.5 | 5854.5 | 69660 | NL |
| 5854.5 | 5874.5 | 68480 | NL |
| 5874.0 | 5894.0 | 67220 | NL |
| 5893.7 | 5913.7 | 67420 | NL |
| 5913.5 | 5933.5 | 69350 | NL |
| 5933.5 | 5953.5 | 70230 | NL |
| 5953.5 | 5973.5 | 71060 | NL |
| 5973.0 | 5993.0 | 68960 | NL |
| 5993.0 | 6013.0 | 69140 | NL |
| 6013.0 | 6033.0 | 68840 | NL |
| 6033.0 | 6053.0 | 71450 | NL |
| 6053.0 | 6073.0 | 71040 | NL |
| 6070.0 | 6090.0 | 71150 | NL |
| 6090.0 | 6110.0 | 71210 | NL |
| 6110.0 | 6130.0 | 72430 | NL |
| 6130.0 | 6150.0 | 71280 | NL |
| 6150.0 | 6170.0 | 70460 | NL |
| 6170.0 | 6190.0 | 73300 | NL |
| 6190.0 | 6210.0 | 73350 | NL |
| 6209.7 | 6229.7 | 72760 | NL |
| 6229.0 | 6249.0 | 71760 | NL |
| 6249.0 | 6269.0 | 72270 | NL |
| 6269.0 | 6289.0 | 73760 | NL |
| 6289.0 | 6309.0 | 72400 | NL |
| 6309.0 | 6329.0 | 73300 | NL |
| 6329.0 | 6349.0 | 73390 | NL |
| 6349.0 | 6369.0 | 74550 | NL |
| 6369.0 | 6389.0 | 75270 | NL |
| 6389.0 | 6409.0 | 73830 | NL |
| 6409.0 | 6429.0 | 73780 | NL |
| 6429.0 | 6449.0 | 74730 | NL |
| 6449.0 | 6469.0 | 74820 | NL |
| 6469.0 | 6489.0 | 75290 | NL |
| 6489.0 | 6509.0 | 73520 | NL |
| 6509.0 | 6529.0 | 75750 | NL |
| 6529.0 | 6549.0 | 75670 | NL |
| 6549.0 | 6569.0 | 65720 | NL |
| 6611.0 | 6631.0 | 76790 | NL |
| 6653.0 | 6673.0 | 76560 | NL |
| 6780.0 | 6800.0 | 75380 | NL |

NOTE:

1. Sources are: SPN = Simon, Pastiels, and Nevejans (1982)
   B = Broadfoot (1972)
   S = Simon (1975)
   NL = Neckel and Labs (1981)

FILE 1 RECORD 951 2000 BYTES

7229-19,7222-19,7247-19,7248-19,7238-19,7239-19,7230-19,7238-19,7232-19,7222-19,7214-19,7214-19,7222-19,7222-19,7230-19,7
230-19,7230-19,7230-19,7222-19,7222-19,7222-19,7206-19,7198-19,7198-19,7206-19,7206-19,7214-19,7214-19,7222-19,7222-19,723
1-19,7230-19,7230-19,7230-19,7230-19,7230-19,7217-19,7198-19,7206-19,7206-19,7206-19,7222-19,7230-19,7230-19,7222-19,7222-
19,7222-19,7222-19,7230-19,7230-19,7238-19,7238-19,7246-19,7246-19,7238-19,7222-19,7214-19,7198-19,7206-19,7207-19,7222-19
7222-19,7222-19,7206-19,7198-19,7198-19,7198-19,7198-19,7181-19,7166-19,7166-19,7182-19,7190-19,7190-19,7190-19,7190-19,7
198-19,7181-19,7166-19,7166-19,7158-19,7158-19,7158-19,7142-19,7150-19,7150-19,7158-19,7158-19,7141-19,7125-19,7109-19,709
3-19,7085-19,7069-19,7069-19,7053-19,7037-19,7021-19,6997-19,6981-19,6973-19,6957-19,6949-19,6933-19,6933-19,6950-19,6982-
19,6997-19,7013-19,7013-19,7021-19,7037-19,7037-19,7037-19,7046-19,7062-19,7069-19,7070-19,7077-19,7061-19,7045-19,7029-19
7029-19,7029-19,7013-19,6997-19,6965-19,6933-19,6893-19,6877-19,6852-19,6804-19,6739-19,6660-19,6563-19,6467-19,6369-19,6
274-19,6170-19,6088-19,6008-19,5961-19,5945-19,5945-19,5977-19,6025-19,6089-19,6170-19,6258-19,6356-19,6444-19,6540-19,661
2-19,6676-19,6708-19,6740-19